Mon. Not. R. Astron. Soc. **282,** 1483–1488 (1996)

ROSAT observations of distant 3CR radio galaxies – II

C. S. Crawford and A. C. Fabian

Institute of Astronomy, Madingley Road, Cambridge CB3 0HA

Accepted 1996 June 30. Received 1996 June 12; in original form 1996 January 5

ABSTRACT

The X-ray emission from high-redshift radio galaxies reveals the properties of their environment, as well as the degree of obscuration of the nuclear component. In this paper we compile and compare all archival *ROSAT* PSPC observations, pointed and serendipitous, of 3CR radio galaxies above a redshift z of 0.4. We present new detections of four galaxies in the redshift range $1 < z < 1.8$, one of which is an 'N galaxy'. Of the three radio galaxies where no optical nucleus is seen, the X-ray emission of one (3C 194) appears to be dominated by an absorbed power-law component; the others (3C 294 and 324) are fitted equally well by either an absorbed power law or a thermal model. The inferred thermal X-ray luminosity is consistent with the radio galaxy being in a moderately rich X-ray cluster of galaxies. If our interpretation is correct, the cluster around 3C 294 at a redshift of 1.786 is the most distant yet detected in X-rays. Our results support a simple model where the X-ray emission from distant objects classified as radio galaxies originates in a hot surrounding intracluster medium, sometimes with the addition of an absorbed power-law component from the central nucleus.

Key words: galaxies: active – galaxies: nuclei – radio continuum: galaxies – X-rays: galaxies.

1 INTRODUCTION

ROSAT observations of powerful radio galaxies have shown that there are two possible components for the X-ray emission. The first is from the active nucleus. In a typical radio galaxy the nucleus is highly obscured, or undetectable, in the optical band, and is similarly expected to be highly absorbed or undetectable in X-rays. Only in broad-line radio galaxies (or those classified as 'N' galaxies) where the nucleus is clearly detected in the optical band is this component expected to be bright and detectable in soft X-rays. Low-redshift examples include 3C 109 (Allen & Fabian 1992) and 3C 287.1 (Crawford & Fabian 1995, hereafter CF95). The second component is emission from a hot surrounding medium, such as provides a working surface on which the jets form the radio lobes. For powerful objects this probably is the intracluster gas in a surrounding cluster of galaxies. There is evidence from optical and radio wavebands that distant powerful radio galaxies (redshift $z > 0.3$) lie at the centre of moderately rich clusters of galaxies (Yates, Miller & Peacock 1989; Hill & Lilly 1991) with a dense intracluster medium (Barthel & Miley 1988; Garrington & Conway 1991).

A good example of a powerful radio galaxy at low redshift showing both components is Cygnus A. The X-ray emission from this is dominated below photon energies of 4 keV by the thermal emission from the surrounding cluster, and above that energy by a heavily absorbed power-law spectrum (column density $\sim 4 \times 10^{23}$ cm^{-2}: Arnaud et al. 1987; Ueno et al. 1994). Only the cluster component would be detectable from such an object at $z \sim 1$ with *ROSAT*, which operates over the 0.1–2.4 keV band. Support for the presence of an X-ray-emitting intracluster medium around powerful distant radio galaxies has been obtained from *ROSAT* X-ray observations of the radio galaxy 3C 356 at $z = 1.08$ (Crawford & Fabian 1993, 1996, hereafter CF93, CF96). X-ray emission is detected with the Position Sensitive Proportional Counter (PSPC) at the softest energies, and thus its X-ray emission cannot be from an obscured active nucleus. A long exposure with the High Resolution Imager (HRI) confirms that the X-ray emission from 3C 356 does not originate from a point-like component (CF96), so that an extended intracluster medium is the likely source.

Most of the X-ray detections and limits of powerful distant 3CR galaxies exceed 10^{44} erg s^{-1}, which rules out many

possible emitting components such as inverse Compton emission from the lobes and starbursts. There is, for example, no sign of any X-ray emission from the widely separated lobes of 3C 356 (CF93; CF96), and the X-ray luminosity of massive starbursts such as Arp 220 is only a few times 10^{41} erg s^{-1} (David, Jones & Forman 1992). Since the bulk of the objects that we are studying have no broad emission lines, we consider only two alternatives for the X-ray emission: a surrounding intracluster medium and a highly absorbed nucleus (column density exceeding 10^{23} cm^{-2}). We also ignore any contribution from unbeamed X-ray emission originating in a jet; for example, the X-ray jet in the nearby radio galaxy. Cen A emits at only 0.1 per cent of the intrinsic X-ray luminosity of the nucleus (Schreier et al. 1979).

Here we examine X-ray observations of other distant radio galaxies in order to assess the relative contribution of the absorbed nucleus and soft intracluster medium. The presence of an intracluster medium around high-redshift radio galaxies has important implications both for its role in influencing the appearance and evolution of radio sources, and for the way in which powerful radio sources act as markers to distant clusters so that the evolution of cluster gas can be studied back well beyond a redshift of unity.

2 THE DATA

We have searched the *ROSAT* data archive for all PSPC observations of 3CR radio galaxies above a redshift of 0.4 (including those classified as N galaxies by Spinrad et al. 1985), and available to the public by 1995 December 4. Both pointed and serendipitous observations were included, except where the optical position of the galaxy lay behind an obscuring support rib, or close to the edge of the field. Investigation of the broad-band images was carried out within the X-ray analysis package XIMAGE. Where no X-ray source was detected coincident with the optical position of the galaxy as given by Spinrad et al. (1985), we quote a 3σ upper limit to the count rate. σ is taken as the square root of the predicted background counts within the detection box, where the background rate is determined from a surrounding annulus that excludes any neighbouring X-ray sources. The source box size is increased for off-axis (serendipitous) observations, in order to allow for variation of the point-spread function (PSF). The count rates are corrected for vignetting off-axis and the spread of the PSF beyond the source detection box, and correspond to the whole *ROSAT* band (0.1–2.4 keV).

Our sample includes three new detections of classical, distant, radio galaxies, all of which are at greater redshifts than the most distant one published previously (3C 356 at $z=1.079$; CF93). They are 3C 294 ($z=1.786$), 3C 194 ($z=1.779$) and 3C 324 ($z=1.2063$); each detection has $\sim$25–35 counts. The detections are all consistent with the PSF of the instrument, although with so few counts it would be difficult to resolve an extent with any certainty. As for our previous study of the PSPC data of 3C 356 (CF93), we have fitted a crude spectrum (binned such that there is a minimum of seven counts per bin) to each of these sources using the software package XSPEC. Fitting spectra to such weak sources is problematic, since a larger spatial bin must be used to extract spectra than is used for source detection. This necessarily reduces the signal-to-noise ratio for spectra relative to that for source detection. Also, we have only a few spectral bins, so that we cannot freely fit over a range of spectral parameters. None of the spectra allow us to confidently distinguish between the thermal emission due to intracluster gas from an absorbed nucleus, except that the quality of the fit for a thermal model to 3C 194 is significantly worse than that of the absorbed power law. We therefore tabulate the results for each model spectra for the four galaxies (Table 1; we assume $H_0=50$ km s^{-1} Mpc^{-1} and $q_0=0.5$ throughout).

We have also studied the data from the N galaxy 3C 208.1 ($z=1.02$), which was detected with $\sim$270 counts. This is well fitted by a power-law spectrum with index $\Gamma\sim2$ and little excess absorption, as expected since the nucleus is detected in the optical band.

Results for all radio galaxies are presented in Table 2. The absorption-corrected, 0.7–2 keV (rest-frame) luminosities of the four galaxies deduced by spectral fitting are listed (in bold font); for the other galaxies in Table 2 this luminosity is inferred from the broad-band counts, again assuming a thermal spectrum of temperature 4 keV and abundance 0.3 solar. The only exceptions are the other two listed as N galaxies (3C 99 and 318), for which we assume a $\Gamma=2$ power-law model. For all galaxies where the luminosity is derived from the count rate, we do not assume any absorption in excess of the Galactic column density, which may

Table 1. Results of spectral fitting.

	Γ	N_H (10^{22} cm^{-2})	χ^2_ν	d.o.f.	L_{PL} (10^{44} erg s^{-1})	χ^2_ν	d.o.f.	L_T (10^{44} erg s^{-1})
3C194	2.0†	16^{+28}_{-13}	1.08	5	38.9	1.48	6	3.5
3C208.1	2.1±0.3	<0.05	0.92	35	7.2	1.06	37	6.2
3C294	2.0†	<19	0.85	6	4.5	0.90	7	1.7
3C324	2.0†	$0.5^{+7}_{-0.5}$	1.92	8	1.6	1.92	9	1.0

†This parameter value fixed.
The power-law (L_{PL}) and thermal (L_T) luminosities are the 0.7–2 keV (rest-frame) luminosities corrected for absorption. N_H is in excess of the Galactic column, and assumes that the absorption is at the redshift of the radio galaxy. The results shown are for fitting the spectrum either by an absorbed power-law (columns 2–6), or by a thermal Raymond–Smith spectrum (abundance 0.3 solar, temperature 4 keV) with no absorption in excess of the Galactic column (columns 7–9).

Table 2. X-ray luminosities of the sample.

3C		z	$\log(N_H)$ (cm^{-2})	ROR	Exposure (sec)	θ (′)	countrate (10^{-3}ct s^{-1})	L_X (10^{44} erg s^{-1})
294		1.786	20.08	RP700117	22692	0	1.12	**1.7**
194		1.779	20.69	RP700049	7945	0	3.84	**3.5***
324		1.2063	20.65	RP701373n00	15434	0	2.07	**1.0**
368		1.132	20.99	RP800394n00	26414	0	0.76	0.6
356		1.079	20.44	RP800395	18565	0	1.54	0.7
208.1	N	1.02	20.55	RP700887n00	18552	26	14.74	**7.2**†
280		0.9975	20.08	RP700073	48051	0	0.91	1.1
277.2		0.766	20.28	RP800393a01	13575	0	0.88	0.2
257		2.474	20.69	RP701377n00	3248	0	< 1.27	< 4.4
256		1.819	20.05	RP700051	6384	0	< 1.29	< 1.4
13		1.351	20.79	RP600244n00	35893	29	< 1.81	< 1.7
210		1.169	20.49	RP701375n00	14767	0	< 0.48	< 0.3
289		0.9674	20.08	RP200749	2616	34	< 10.13	< 3.0
263.1		0.824	20.32	RP701149n00	4889	31	< 7.02	< 1.7
114		0.815	21.24	RP200442	20241	25	< 2.24	< 1.0
41		0.794	20.72	RP600254a01	15290	39	<3.76	<1.1
318	N	0.752	20.59	RP201179	1210	30	< 9.52	<6.6†
343.1		0.750	20.42	RP701171n00	4831	29	< 4.68	<1.0
220.3		0.685	20.53	RP700072	8791	0	< 3.81	< 0.7
337		0.635	20.02	RP800259	2994	31	< 8.07	< 1.0
330		0.550	20.47	RP700320	8442	30	< 4.36	< 0.5
200		0.458	20.56	RP201083n00	2744	35	< 8.54	<0.7
99	N	0.426	21.02	RP900140	7909	29	< 3.72	<0.4†

N_H quoted in column 4 is the Galactic column density along the line of sight, taken from Stark et al. (1992). θ is the off-axis distance of the optical position of the galaxy, expressed in arcmin. The 1σ uncertainty on the detected count rates of the detected radio galaxies (non-N) is $\sim$20 per cent. The luminosity (L_X) is a 0.7–2 keV (rest-frame) unabsorbed luminosity, assuming a thermal spectrum of temperature 4 keV and abundance 0.3 solar.
†Where the 3C object is marked as an 'N' galaxy in column 2, the quoted luminosity (L_X) assumes a power-law spectrum with $\Gamma = 2$.
Those luminosities in bold font are taken from spectral fits to the data; all others are inferred from the broad-band number counts.

lead to the limit on the two N galaxies in particular being underestimated. As we do not use the true distribution of these counts across the band (and thus have to assume both that there is no excess absorption, and that the spectrum used is appropriate), the uncertainty on these luminosities could be as high as $\pm$50 per cent.

We quote 0.7–2 keV luminosities, as this band covers the rest-frame energies common to all our sample in the observed PSPC 0.1–2.4 keV band. (For our adopted thermal spectrum, this band carries 30 per cent of the total flux, whereas the 0.1–2.4 and 2–10 keV bands carry 60 and 46 per cent respectively). The majority of galaxies in our sample have only upper limits to the X-ray flux emitted at the optical position of the galaxy; either the exposures are short, or the source position is well off-axis, which degrades the PSF and sensitivity and thus the detection rate. We include rederived luminosities of radio galaxies from our previous papers (3C 277.2, 356 and 368; CF93, CF95), as well as those observed by Worrall et al. 1994 (3C 220.3 and 280) to create a uniformly derived sample (luminosities were previously quoted in the 0.1–2.4 keV observed frame). Although Worrall et al. indicate that the spatial profile of 3C 280 can be decomposed into a point-like and an extended component, we do not attempt here to split the luminosity of 3C 280 into separate origins.

The luminosities for the four detected objects are obtained from a region of about 1-arcmin radius ($\sim$500 kpc for a source at $z \sim 1$–2); for the remainder, in order to optimize the signal-to-noise ratio, we use a box centred on the source of side 32 arcsec, with the luminosity scaled from that as for an unresolved point source. Since the X-ray half-light radii of nearby clusters is about 200 kpc when there is a central cooling flow (and significantly larger when there is not), the luminosities apply only to the notional cluster core and cooling flow (if present). It is therefore possible that we have underestimated the total X-ray luminosities by 50 per cent for the thermal components of 3C 194, 294 and 324, and by 100 per cent or even more for the remainder. The precise value depends on the (unknown) X-ray surface brightness profiles of distant clusters.

We plot the 0.7–2 keV luminosity of the radio galaxies against redshift in Fig. 1, assuming they all have a thermal spectrum (excluding the N galaxies 3C 99 and 318). Only the upper limits to the thermal component luminosity from the combined fit to 3C 208.1 and 194 are plotted. (We emphasize that this plot differs from that in fig. 6 of CF95,

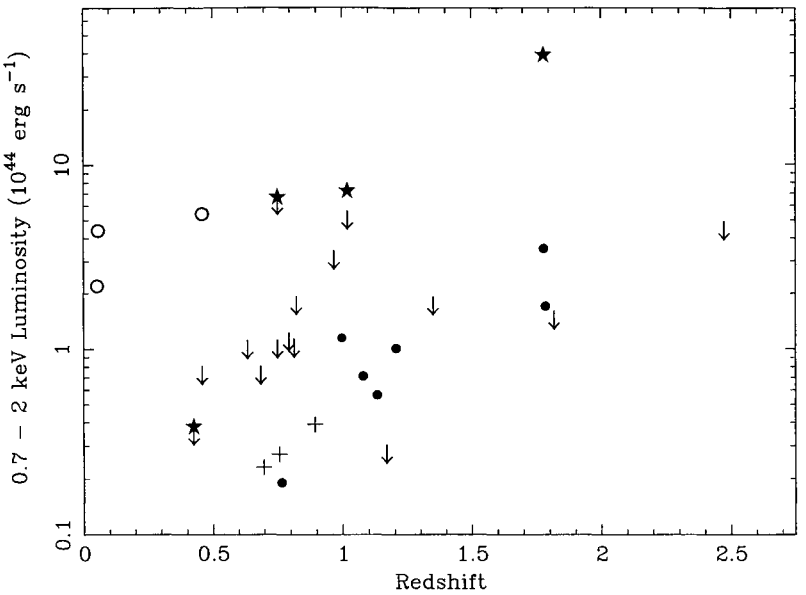

Figure 1. The unabsorbed rest-frame 0.7–2 keV luminosity plotted as a function of redshift for all the radio galaxies in Table 2. Detected radio galaxies are marked as filled circles, the N galaxies are marked by stars, and optically selected clusters (from Castander et al. 1994) as crosses. Broad-beam X-ray luminosites of Cygnus A (left upper), Hydra A (left lower) and 3C 295 (right) are marked by open circles; note that the luminosity in these clusters within the inner 150–500 kpc (i.e., a similar region to that used for detecting the distant emission) is a factor of 1/2 to 2/3 smaller than that shown here. The uncertainties due to (a) counting statistics on the detected sources (± 20 per cent), and (b) source extent or intrinsic absorption mean that the total emitted luminosities are underestimated, and could be up to a factor of 2 higher.

in that we are now comparing the same rest-frame luminosity of the galaxies, instead of the observed 0.1–2.4 keV luminosity). Note that uncertainties due to the extent of the clusters and any intrinsic absorption mean that we are showing lower limits for the detected objects. Included for comparison are the luminosities of the highest redshift, optically selected clusters detected in X-rays (Castander et al. 1994), the X-ray luminosities of the clusters associated with the strong, low-redshift radio sources, Cygnus A and Hydra A [open circles – note that the *core* luminosities of these clusters is about 1/2–2/3 of the plotted value, thus $\sim(1.5\text{–}3)\times10^{44}$ erg s^{-1}; for details of the X-ray properties of these clusters, see David et al. 1990 and Reynolds & Fabian 1996] and of the cluster around 3C 295 at $z=0.46$ (Henry & Henricksen 1986).

3 DISCUSSION

Of the newly detected radio galaxies, 3C 294 and 324, are well-known examples of the 'alignment effect' between the optical continuum and the radio source axis (McCarthy 1993, and references therein). 3C 324 has a large surrounding emission-line nebula (Spinrad & Djorgovski 1984), and is known from *HST* images and follow-up spectroscopy to have several galaxies at the same redshift (Dickinson, private communication). X-ray emission from a cluster at the same redshift is therefore highly plausible. 3C 294 has an excess of objects detected in *R*-band imaging (Benitez, Martinez-Gonzalez & Gonzalez-Serrano 1995) and a spectacular Lyα halo, extending over a region of about 170×100 kpc^2 (McCarthy et al. 1990). It is also highly depolarized in the radio (Liu & Pooley 1991), which is a signature of a hot intracluster medium, and of a cooling flow if comparison is made with low-redshift objects (Taylor et al. 1994; Fabian et al. 1986 previously noted the similarity between the optical appearance of distant powerful radio galaxies and strong nearby cooling flows). Less is known about the optical appearance of 3C 194, although Djorgovski et al. (1988) suggest that its properties are similar to those of 3C 294. 3C 194 is the only high-redshift (non-N) radio galaxy so far detected by *ROSAT* with an X-ray spectrum better fitted by an absorbed power law. Its radio depolarization (Taylor, Inoue & Tabara 1992) does, however, indicate that a thermal component should be present. The nucleus of 3C 194 should be detectable in the infrared.

The 0.7–2 keV X-ray luminosities of the cores of 3C 280, 294, 324, 356 and 368 are all within the range $(0.5\text{–}1.7)\times10^{44}$ erg s^{-1} and easily compatible with the X-ray luminosity expected from a moderately rich cluster of galaxies. Fig. 1 shows that the X-ray emission is comparable to that from the core of the cluster surrounding the low-redshift radio source Hydra A, and only slightly less luminous than that associated with Cygnus A. The upper limits to the X-ray emission for the non-detected radio galaxies are all compatible with this luminosity range, except 3C 210 which is significantly lower (see the lower limit in Fig. 1 lying at a redshift of 1.17, below the X-ray-detected radio galaxies). We do not know why it is an exception.

The X-ray emission from 3C 208.1 is well fitted by a power-law spectrum, with little or no excess absorption, consistent with its classification as an N galaxy, i.e., with the nuclear emission barely hidden at all wavebands. Where a power-law origin for the X-ray emission is deduced from the

spectrum of 3C 194, it is absorbed by a column density in excess of that along the Galactic line of sight. The intrinsic nuclear luminosities of both these galaxies are compatible with those of radio-loud quasars (Worrall et al. 1987), supporting the interpretation of the radio galaxies as misdirected quasars (Barthel 1989). The high excess column density observed for 3C 194 suggests that we observe its nuclear emission through an obscuring torus, and thus perhaps that its axis is pointed further away from our line of sight than is 3C 208.1. 3C 194 and 208.1 have noticeably higher X-ray count rates than the other detected distant radio galaxies, strengthening our supposition that only these two show the power-law contribution to their X-ray emission. Particular comparison can be drawn between 3C 194 and 294, which lie at very similar redshifts; the luminosity limit to the thermal component alone of 3C 194 is very similar to the total luminosity of 3C 294.

If the X-ray emission associated with 3C 294 is thermal in origin, at $z=1.786$ it represents the most distant cluster yet detected in X-rays. If the intracluster medium were of lower temperature than the 4 keV we have assumed in our modelling, it could contain a cooling flow of order $\sim 500\ M_\odot\ yr^{-1}$, or even greater if the thermal emission was itself subject to absorption (see Fabian 1994, and note that a 0.7–2 keV luminosity of 10^{44} erg s^{-1} corresponds to $250\ M_\odot\ yr^{-1}$ cooling from 4 keV, and $\sim 500\ M_\odot\ yr^{-1}$ cooling from 2 keV, both without excess absorption). Note that strong cooling flows are detected in X-rays around Cygnus A (Reynolds & Fabian 1996) and 3C 295 (Henry & Henricksen 1986; Fabian & Crawford 1995). X-ray observations at high spatial resolution, such as will be possible with *AXAF*, are needed to make further direct progress.

We chose radio galaxies as targets to mark the sites of distant clusters of galaxies in order to limit the contamination of X-ray emission from any active nucleus (such as will dominate the emission from radio-loud quasars). Beyond establishing the presence of clusters at high redshifts, we ultimately wish to relate the properties of the environment to those of the radio source – whether the radio sources lying in richer environments show a larger depolarization asymmetry, or a more distorted or compressed morphology. With our current sample we find no clear trend of cluster luminosity with the arm-length asymmetry or core/extended radio power, or the size of the radio source (normalized for a core radio power). A much larger sample of detected objects is required to draw firm conclusions, as many of these other parameters are known to be redshift-dependent.

Although the cluster around Cygnus A is a factor of about 2 times more X-ray-luminous than the emission detected from 3C 294, it is possible that a significant fraction of that difference lies beyond the immediate core of the cluster. Later merging of subclusters with the 3C 294 cluster may enhance the total X-ray luminosity, chiefly by adding gas to the outer parts of the cluster. If much of the emission detected by *ROSAT* is from a strong cooling flow in the inner 100 kpc radius about the radio galaxy, then X-ray absorption as detected in many nearby clusters (see, e.g., White et al. 1991 and Allen et al. 1995) may be important in making the immediate surroundings of Cygnus A and 3C 294 much more similar in total luminosity. Clumps formed in rapidly cooling gas can then help to explain some of the bending, asymmetries and knots of the radio and optical structures commonly seen around distant radio galaxies.

4 CONCLUSIONS

Powerful distant radio galaxies are markers for the X-ray detection of high-redshift clusters of galaxies. The thermal X-ray luminosities of the cores of the host clusters are consistent with those of moderately rich nearby clusters. It is possible that they contain moderate-to-strong cooling flows.

ACKNOWLEDGMENTS

We are grateful to members of the IoA X-ray Group, and in particular Roderick Johnstone, for software management effort. ACF and CSC acknowledge the support of the Royal Society and a PPARC Advanced Fellowship respectively. This research has made use of data obtained through the High Energy Astrophysics Science Archive Research Center Online Service, provided by the NASA-Goddard Space Flight Centre.

REFERENCES

Allen S. W., Fabian A. C., 1992, MNRAS, 258, 29P
Allen S. W., Fabian A. C., Edge A. C, Bohringer H., White D. A., 1995, MNRAS, 275, 741
Arnaud K. A. et al., 1987, MNRAS, 227, 241
Barthel P. D., 1989, ApJ, 336, 606
Barthel P. D., Miley G., 1988, Nat, 333, 319
Benitez N., Martinez-Gonzalez E., Gonzalez-Serrano J. I., 1995, AJ, 109, 935
Castander F. J., Ellis R. S., Frenk C. S., Dressler A., Gunn J. E., 1994, ApJ, 424, L79
Crawford C. S., Fabian A. C., 1993, MNRAS, 260, L15 (CF93)
Crawford C. S., Fabian A. C., 1995, MNRAS, 273, 827 (CF95)
Crawford C. S., Fabian A. C., 1996, MNRAS, 281, L5 (CF96)
David L. P., Arnaud K. A., Forman W., Jones C., 1990, ApJ, 356, 32
David L. P., Jones C., Forman W., 1992, ApJ, 388, 82
Djorgovski S., Spinrad H., McCarthy P., Dickinson M., van Breugel W., Strom R., 1988, AJ, 96, 836
Fabian A. C., 1994, ARA&A, 32, 277
Fabian A. C., Crawford C. S., 1995, MNRAS, 274, L63
Fabian A. C., Arnaud K. A., Nulsen P. E. J., Mushotzky R. F., 1986, ApJ, 305, 9
Garrington S. T., Conway R. G., 1991, MNRAS, 250, 198
Henry J. P., Henriksen M. J., 1986, ApJ, 301, 689
Hill G. J., Lilly S. J., 1991, ApJ, 367, 1
Liu R., Pooley G., 1991, MNRAS, 249, 343
McCarthy P. J., 1993, ARA&A, 31, 639
McCarthy P. J., Spinrad H., Van Bruegel W., Liebert J., Dickinson M., Djorgovski S., Eisenhardt P., 1990, ApJ, 365, 487
Reynolds C. S., Fabian A. C., 1996, MNRAS, 278, 479
Schreier E. J., Feigelson E. D., Delvaille J., Giacconi R., Grindlay J., Schwartz D. A., Fabian A. C., 1989, ApJ, 234, L39
Spinrad H., Djorgovski S., 1984, ApJ, 280, L9
Spinrad H., Djorgovski S., Marr J., Aguilar L., 1985, PASP, 97, 932
Stark A. A., Gammie C. F., Wilson R. W., Bally J., Linke R. A., Heiles C., Hurwitz M., 1992, ApJS, 79, 77
Taylor G. B., Inoue M., Tabara H., 1992, A&A, 264, 415

Taylor G. B., Barton E. J., Ge J. P., 1994, AJ, 107, 1942
Ueno S., Koyama K., Nishida M., Yamauchi S., Ward M. J., 1994, ApJ, 431, L1
White D. A., Fabian A. C., Johnstone R. M., Mushotzky R. F., Arnaud K. A., 1991, MNRAS, 252, 71
Worrall D. M., Giommi P., Tananbaum H., Zamorani G., 1987, ApJ, 313, 596
Worrall D. M., Lawrence C. R., Pearson T. J., Readhead A. C. S., 1994, ApJ, 420, L17
Yates M. G., Miller L., Peacock J. A., 1989, MNRAS, 240, 129